EXPERIMENTAL STUDY ON SEISMIC DAMAGE BEHAVIOR OF STEEL REINFORCED CONCRETE COUPLING BEAMS

State Key Laboratory Research Program

Principal Investigator: Huanjun Jiang (Professor), Tongji University
Student Investigators: Yinghui Li (PhD candidate), Tongji University
Multi-function Vibration Test Center, Tongji University

Introduction

Steel Reinforced Concrete (SRC) coupling beams provide an alternative to reinforced concrete coupling beams and offer potential advantages of reduced section depth, reduced congestion at the wall boundary region, improved degree of coupling for a given beam depth, and improved deformation capacity.

Three full-scale, flexure-yielding, cantilever SRC coupling beams embedded into reinforced concrete structural rigid bases were tested by applying quasi-static, reversed-cyclic loading to the middle span of the coupling beams. The test setup and specimen are illustrated in Figure 1. The principal damage states were also investigated throughout the entire testing process.

Figure 1. Test setup and specimen

Experimental program

Three full sized specimens were designed with different types of cross-section of encased steel and shear studs were attached on the encased steel according to Chinese current codes. The encased steel and bar details are shown in Figure 2. The steel ratio of three specimens is 5% and the span-depth ratio is 2. The main difference among three specimens is the ratio of flange area to web area of encased steel.

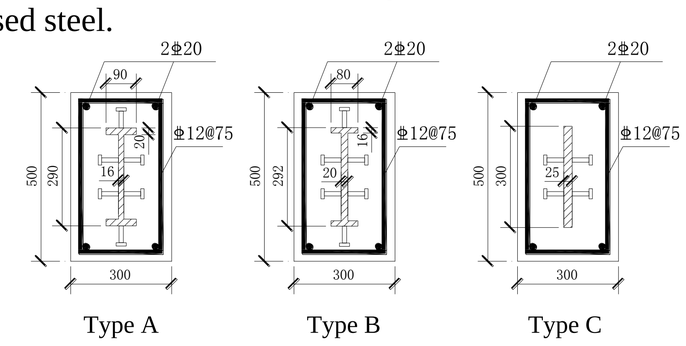

Type A Type B Type C

Figure 2. Encased steel and bar details (unit: mm)

The actual strengths of concrete, steel plate and steel bars were obtained via material property tests. The cubic compressive strength of concrete was 57.5 MPa. The properties of encased steel plate and steel rebar are shown in Tables 1.

Table 1. Properties of encased steel and steel rebar.

Steel rebar or plate	Yielding strength (MPa)	Ultimate strength (MPa)	Elastic modulus (MPa)
Rebar-12	457.0	555.6	190000
Rebar-20	437.5	582.8	196000
Plate-16	249.1	411.2	195000
Plate-20	282.0	452.9	206000
Plate-25	255.0	409.5	206000

When the tension strain of the steel reached the yielding strain, the specimens were regarded as yielding. Prior to the yielding of the specimen, the lateral load was exerted by the force-controlled mode. After the yielding of the specimen, three cycles of loading and unloading were conducted for each following displacement level, increasing in multiples of specimen yielding displacement.

Experimental results

Overview

The sequences of observed damage were similar for the three specimens. The typical damage development of specimen A at different loading stage is shown in Figure 3. The typical development of damage is as follows: horizontal and diagonal cracking of concrete cover, tension yielding of the extreme encased steel and longitudinal bars, crushing of concrete cover, concrete spalling, buckling of longitudinal bars, breaking of longitudinal bars and then fracture of encased steel plates.

The specimens have the similar crack patterns which are shown in Figure 4. The damage development and crack pattern of specimens imply the specimens damage is flexure dominant.

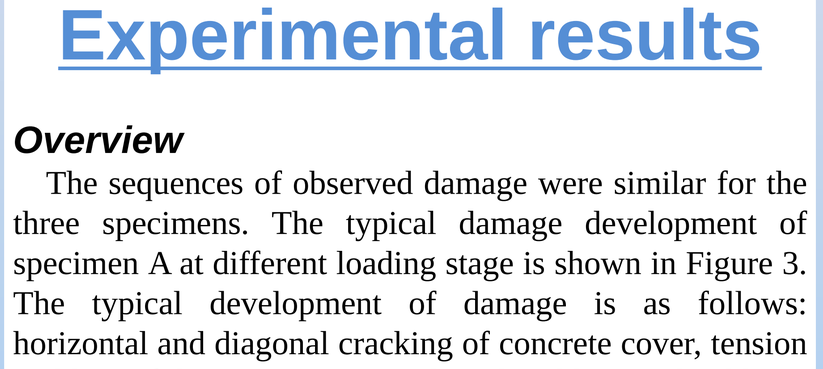

Figure 3. Damage development of specimen A

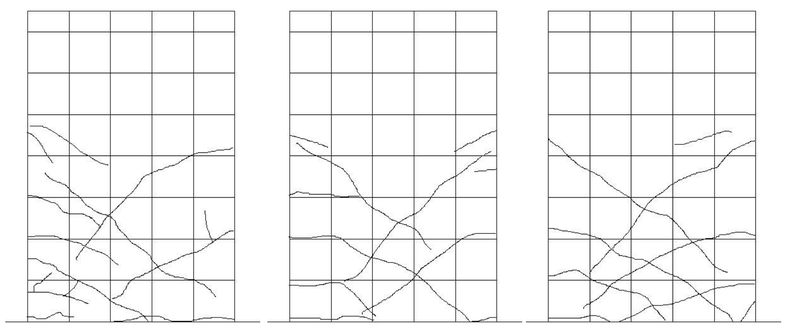

(a) Specimen A (b) Specimen B (c) Specimen C

Figure 4. Crack patterns of specimens

Hysteresis Behavior

Hysteretic curves and corresponding skeleton curves of lateral load vs. the top displacement for the three specimens are plotted in Figure 5. The hysteretic loop of specimen A is fatter than the other two specimens, which means specimen A can consume more energy during the earthquake. The load capacity of specimen B is 20% larger than specimen C and 3% larger than specimen A.

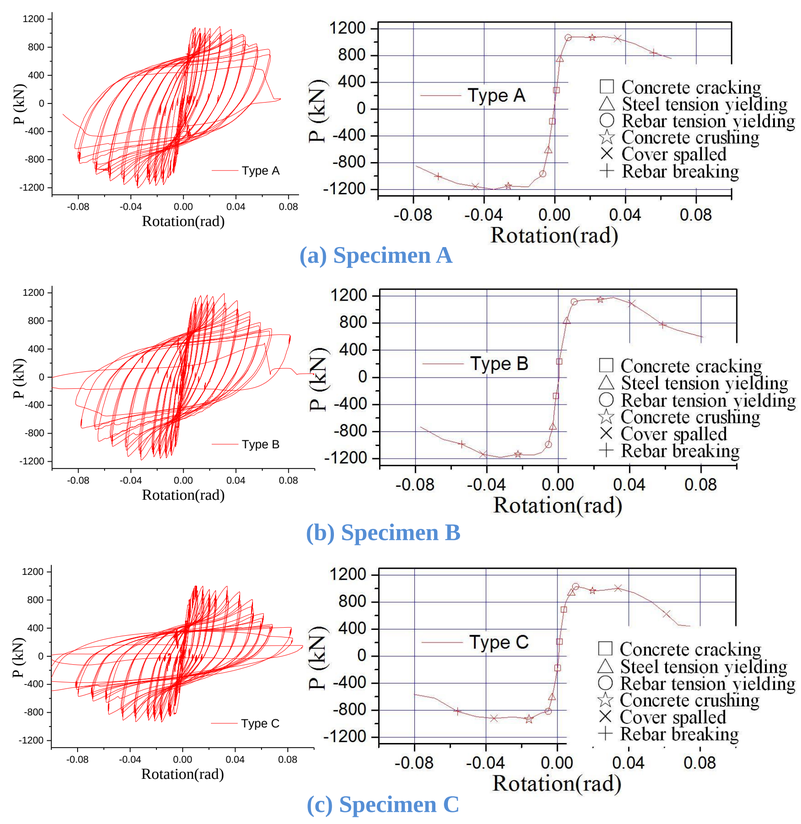

Figure 5. Force-displacement curves of specimens

Ductility Evaluation

In this study. the yielding displacement was determined by the intersection of the horizontal line at the peak force with the straight line passing through the origin and the 75% peak force point on the envelope curve. The ultimate state was defined by the point on the descending section of the envelope curve with 15% force degradation.

The ductility of each specimen was computed for two opposite loading directions, and the mean value was taken as the ductility of the specimen. Table 2 lists the displacement ductility coefficients for three specimens.

The ductility coefficient of specimen B is 24% smaller than specimen C and 19% smaller than specimen A.

Table 2. Displacement ductility coefficient.

Specimen number	Yielding rotation		Ultimate rotation		Ductility coefficient		
	Positive	Negative	Positive	Negative	Positive	Negative	mean
Specimen A	0.0048	-0.0083	0.050	-0.064	10.41	7.71	9.06
Specimen B	0.0072	-0.0063	0.046	-0.053	6.39	8.41	7.40
Specimen C	0.0060	-0.0051	0.048	-0.058	8.00	11.37	9.69

Conclusions

1) Detailed damage state were recorded during the quasi-static test of SRC coupling beams.
2) The damage development, hysteretic behavior and ductility evaluation were analyzed for three SRC coupling beams with different encased steel.
3) SRC coupling beams with steel type A was recommended for practical engineering application for its better energy dissipation capacity, load carrying capacity and ductility.